

A Study of the Effect of Oxygen Plasma Treatment on the Interfacial Properties of Carbon Fiber/Epoxy Composites

Keming Ma,^{1,2} Ping Chen,¹ Baichen Wang,² Guiling Cui,² Xinmeng Xu³

¹Liaoning Key Laboratory of Polymer Science and Engineering, School of Chemical Engineering, Dalian University of Technology, Dalian 116012, China

²Liaoning Key Laboratory of Advanced Polymer Matrix Composites Manufacturing Technology, Shenyang University of Aeronautics and Astronautics, Shenyang 110034, China

³Shenyang Zijiang Package Co., Ltd., Shenyang 110027, China

Received 15 September 2009; accepted 29 March 2010

DOI 10.1002/app.32549

Published online 3 June 2010 in Wiley InterScience (www.interscience.wiley.com).

ABSTRACT: In this work, effects of the interface modification on the carbon fiber-reinforced epoxy composites were studied. For this purpose, the surface of carbon fibers were modified by oxygen plasma treatment. The surface characteristics of carbon fibers were studied by X-ray photoelectron spectroscopy (XPS), atomic force microscopy (AFM), dynamic contact angle analysis (DCAA), and dynamic mechanical thermal analysis (DMTA), respectively. The interlaminar shear strength (ILSS) was also measured. XPS and AFM analyses indicated that the oxygen plasma treatment successfully increased some oxygen-containing functional groups concentration on the carbon

fiber surfaces, the surface roughness of carbon fibers was enhanced by plasma etching and oxidative reactions. DCAA and DMTA analyses show that the surface energy of carbon fibers increased 44.9% after plasma treatment for 3 min and the interfacial bonding intensities A and α also reached minimum and maximum value respectively. The composites exhibited the highest value of ILSS after oxygen plasma treated for 3 min. © 2010 Wiley Periodicals, Inc. *J Appl Polym Sci* 118: 1606–1614, 2010

Key words: interface; cold plasma treatment; atomic force microscopy (AFM); XPS; DMTA

INTRODUCTION

Advanced polymer composites have been widely utilized in structural applications due to their high specific strength and stiffness, good corrosion resistance and low thermal expansion relative to conventional metallic materials. However, composite materials also have certain drawbacks such as poor interfacial adhesion between the reinforcement and the matrix resin, which is a critical factor in the properties of composite materials. The mechanical performance of composite materials depends not only on the matrix and the reinforcing fiber properties, but also to a great extent on the fiber/matrix adhesion. To improve the adhesion between the fiber and matrix, it is necessary to increase the fiber's surface polarity, create more

sites for hydrogen bonding and improve the possibility for mechanical interlocking between fiber materials and the surrounding matrix materials, which lead to good stress transfer from the matrix materials to the fiber ones.

Carbon fibers combine exceptional mechanical properties and low weight, making them ideal reinforcements for polymer matrix composite materials. However, the carbon fiber surface is smooth and has low polarity, which makes it difficult to wet, while the lack of reactive functional groups on the surface makes it difficult to form chemical bonds with the matrix resin,^{1–4} to improve the fiber-matrix adhesion, many surface treatment techniques were developed, including γ -ray radiation, electrochemically oxidation, plasma treatment, ozone (O₃) treatment, etc.^{5–14} The application of cold plasma in the treatment of carbon fibers has become increasingly important. Plasma treatment modifies the uppermost atomic layer of the material surface without affecting its bulk characteristics.¹⁵

In this study, the oxygen plasma treatment method was adopted to modify the surface of the carbon fiber and the effects of oxygen plasma treatment on the interface and mechanical properties were investigated. The characterization of oxygen plasma treatment of fibers is discussed here to

Correspondence to: P. Chen (chenping_898@126.com).

Contract grant sponsor: National Natural Science Foundation of China; contract grant number: 50703024.

Contract grant sponsor: Innovative Research Team Program (University of Liaoning Education Department); contract grant numbers: 2006T109, 2008T148.

Contract grant sponsor: Program for Liaoning Excellent Talents in University; contract grant number: 2008RC39.

TABLE I
Chemical Structures of the Materials

Materials	Chemical structures
DGEBA	
DGEAC	
2-Ethyl-4-methylimidazole	

obtain a better understanding of the interfacial adhesion mechanism. The characterization was carried out by XPS, AFM, dynamic contact angle analysis (DCAA), dynamic mechanical thermal analysis (DMTA), and interlaminar shear strength (ILSS) measurements, and the results were correlated to the interfacial adhesion results.

EXPERIMENTAL

Materials

Two types of epoxy resins were used in this study. The diglycidyl ether of bisphenol A (DGEBA) type epoxy resin was supplied by Yueyang Resin Factory (epoxy value 0.51), the diglycidyl ester of aliphatic cyclohexane (DGEAC) type epoxy resin was provided by Tianjin Jindong chemical factory (epoxy value, 0.85).

2-Ethyl-4-methylimidazole, obtained from Shanghai Jingchun Reagents (Shanghai, China), was used as curing agent.

The chemical structures of the resins and curing agent are shown in Table I.

The epoxy resin matrix was prepared with DGEAC and DGEBA at a ratio of 100 : 30 and the curing agent was 3 phr (parts for 100 parts of resin) of 2-ethyl-4-methylimidazole. The mixture was heated and stirred for the complete dissolution of curing agent in the epoxy resin for 20 min at 50°C.

The carbon fibers used in this study were PAN-based T700SC produced by Toray, Japan (12×10^3 single filaments per tow, tensile strength was 4.9 GPa, tensile modulus was 230 GPa, average diameter was about 7 μm and elongation was 2.1%). The fibers were extracted with acetone at room temperature for about 24 h to remove surface sizing or contaminants. The fiber samples were then dried at 110°C in a vacuum oven for 3 h before oxygen plasma treatment.

Plasma treatment

The plasma treatment was conducted in an inductive coupling radio frequency (13.56 MHz) plasma

reactor with a power source of 1000 W. The treatment system is composed of a vacuum chamber, three mass flow controllers, a pressure gauge, a pumping system and a radio source. The pumping system is composed of a mechanical pump and a turbine molecular pump. Oxygen was fed into the vacuum chamber at a flow rate of about 6–8 SCCM. The operation pressure was set at 15 Pa. Carbon fiber tows were carefully wrapped around a glass frame and treated by oxygen plasma for 1, 3, 5, and 7 min, respectively, under a power of 300 W.

Composites preparation

Carbon/epoxy composites were manufactured by compression molding technique. The untreated and plasma-treated carbon fiber tows were impregnated by passing them through an epoxy resin matrix bath at 50°C. Two glass bars were used to scrape off excess epoxy resin from the fiber tows carefully.

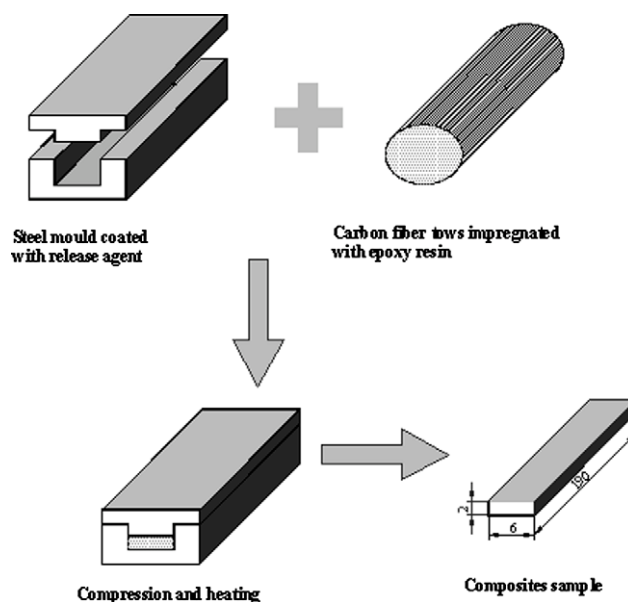


Figure 1 Fabrication procedure of the unidirectional composites.

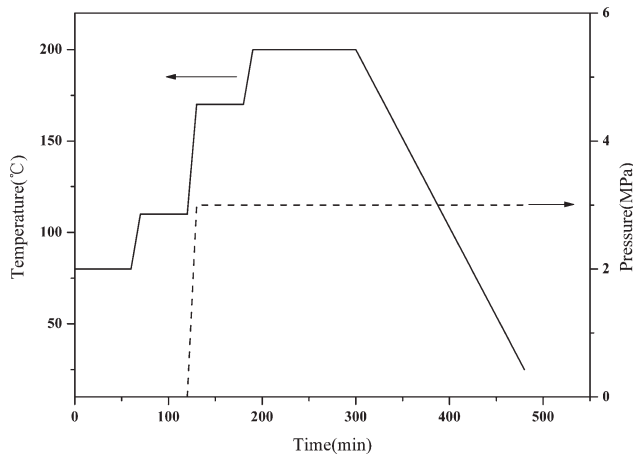


Figure 2 Molding cycle of carbon/epoxy composites.

Sixteen carbon fiber tows were laid parallel to each other in the concave die and inserted into the convex die (see Fig. 1). The molding cycle is represented in Figure 2. All composites samples were about 6 mm in width and 2 mm in thickness, the fiber volume fraction of bulk specimens was 40.32–53.22%.

Dynamic contact angle analysis

The surface free energy and contact angles of carbon fibers were measured by a Cahn DCA-322 (Thermo) DCAA system. The fiber sample was cut into 10 mm in length and mounted indirectly to a wire hook suspended from a microbalance of the DCAA system. When the fiber sample was immersed into the testing liquids at equilibrium, the net force (F_{Measured}) acting on the fiber sample is made up of the gravitational force (F_{Fiber}), the sum of the wetting (F_{Wetting}) and the buoyancy force (F_{Buoyancy}), as shown in the following equation:

$$F_{\text{Measured}} = F_{\text{Fiber}} - F_{\text{Buoyancy}} + F_{\text{Wetting}} \quad (1)$$

By moving the elevating stage up to the fixed immersion depth at a constant speed of 1 mm/min, a typical force-high plot was obtained schematically. The dynamic contact angle (θ) was calculated from the following equation:

$$F_{\text{Wetting}} = \gamma p \cos \theta \quad (2)$$

where γ stands for surface tension of the testing liquids, p stands for the wetted perimeter, and θ is the dynamic contact angle between fiber and the testing liquids.

Fiber surface free energy, which can be divided into two components: dispersive component and polar component, were derived from the following equations:

$$\gamma_l(1 + \cos \theta) = 2\sqrt{\gamma_s^p \gamma_l^p} + 2\sqrt{\gamma_s^d \gamma_l^d} \quad (3)$$

$$\gamma_s = \gamma_s^p + \gamma_s^d \quad (4)$$

where γ_l stands for surface tension of the testing liquid, γ_s stands for total surface free energy of the fiber, γ_s^p and γ_s^d are the polar component and the dispersive component of the total surface free energy.^{16–18} The testing liquids used in the measurement were water (polar solvent) and diiodomethane (nonpolar solvent), their surface tension were 72.3 mN/m and 50.8 mN/m, respectively. The contact angles of each specimen was averaged with five successful measurements.

X-ray photoelectron spectroscopy (XPS)

XPS analysis was used to determine the chemical changes on the carbon fiber surfaces introduced by plasma treatment. XPS measurements were carried out on a XPS (ESCALAB 250, Thermo). The XPS spectra were obtained using Al K_{α} ($h\nu = 1486.6$ eV) monochromated X-ray source with a voltage of 15 kV and a power of 150 W. The XPS measurements were performed at an operating vacuum better than 3.0×10^{-9} mbar. Spectra are acquired at a take-off angle of 90° relative to the sample surface. The pass energy and energy step were 20 eV and 0.1 eV, respectively. The nonlinear least squares fitting (NLLSF) program with a Gaussian-Lorentzian production function was used for curve fitting of C1s spectra. The surface chemical composition was calculated from the areas of relevant spectra peaks.

Atomic force microscopy (AFM)

Surface roughness and surface morphologies of carbon fibers were characterized by AFM (PicoScanTM 2500, MI). Two or three carbon fiber filaments were fastened to a steel sample mount. A tapping mode was used to scan the fiber surface. AFM images of CF were obtained with a force constant of about 0.4 N/m and a scan area of $4 \mu\text{m} \times 4 \mu\text{m}$.

Interlaminar shear strength

The interfacial adhesion between fiber and matrix resin was measured by the short beam three point bending test (ASTM D-2344). The apparatus used was an Instron 5567, the width of the test specimen was 6 mm and the thickness was 2 mm. The ILSS of composites was calculated according to the following equation. A span-to-depth ratio of 5 : 1 and a cross-head speed of 2 mm/min were used. The ILSS of each specimen was averaged with five values.

$$\text{ILSS} = \frac{3P_b}{4bh} \quad (5)$$

where, P_b is the maximum compression load at fracture in Newtons, b is the breadth of the specimen in mm, and h is the thickness of the specimen in mm.

TABLE II
Surface Chemical Composition of Carbon Fibers

Samples	Relative concentration of elements (%)			O/C
	C	O	N	
Untreated	85.5	13.2	1.3	0.15
Plasma treated for 1 min	84.6	14.5	1.0	0.17
Plasma treated for 3 min	79.9	20.1	0	0.25
Plasma treated for 5 min	82.4	17.1	0.6	0.21
Plasma treated for 7 min	87.9	11.0	1.2	0.13

Dynamic mechanical thermal analysis

DMTA was conducted with Pyris DMA 7e Dynamic Mechanical Analyzer (Perkin-Elmer) to obtain the loss factor $\tan\delta$ for both untreated and Plasma treated composites.

Rectangular specimens, with a dimension of $30 \times 6 \times 1$ mm were heated up to 250°C from room temperature with a heating rate of $2^\circ\text{C}/\text{min}$. The measurements were carried out using the three point bending method with an oscillating frequency of 1 Hz.

For the composites, the initial modulus value is the one resulting from the sum of factors, such as matrix and fiber types, fiber portion, stiffness of one and the other phase, and the number of existing matrix-fiber links. So the differences observed experimentally can be explained in terms of fiber treatment and the existence of matrix-fiber links. The effect of the interfacial region on the dynamic properties can be quantified fairly accurately with interfacial bonding intensities factors A and α , which were derived from the following equations:¹⁹

$$A = \frac{1}{1 - V_f} * \frac{(\tan\delta_{\max})_c}{(\tan\delta_{\max})_m} - 1 \quad (6)$$

$$(\tan\delta_{\max})_c = (\tan\delta_{\max})_m - \alpha V_f \quad (7)$$

where, the subscripts f , c , and m refer to the fiber, the composites, and the matrix, respectively, and V is the volume fraction. A low A value and high α value is indicative of a high degree of fiber-matrix interaction or adhesion at the interface.

RESULTS AND DISCUSSION

Surface chemical composition of carbon fibers

The surface composition of untreated and oxygen plasma treated carbon fiber is given in Table II. It was found that the carbon concentration declined after oxygen plasma treatment. Oxygen concentration increased from 13.2% to 20.1% and the ratio of oxygen to carbon atoms increased notably from 0.15 to 0.25 after oxygen plasma treatment for 3 min due to

the increase in oxygen-containing functional groups on the carbon fiber surfaces. However, when the plasma treatment time increased from 3 min to 7 min, the oxygen concentration and the ratio of oxygen to carbon atoms decreased from 20.1% to 11.0% and 0.25 to 0.13, respectively.

To investigate what chemical functional groups are introduced onto the carbon fiber surface after oxygen plasma treatment, deconvolution analysis of C1s peaks was performed. The C1s XPS spectra of untreated and the oxygen plasma treated carbon fiber surfaces are revealed in Figure 3. As well documented in literature,^{4-8,10} a maximum of five peaks were needed to fit the C1s signal properly. The peak assignment can be made as follows: $-\text{C}-\text{C}-$ at 284.6 eV; $-\text{C}-\text{N}$ at 285.4 eV; $-\text{C}-\text{OH}/-\text{C}-\text{O}-\text{C}$ at 286.1–286.7 eV; $-\text{C}=\text{O}$ at 286.6–287.9 eV; $-\text{COOH}/-\text{COOR}$ at 288.2–289.1 eV and $-\text{COO}^-/\text{CO}_2/\pi \rightarrow \pi^*$ shake-up at 290.1–291.5 eV. The spectrum intensity and peak areas of the untreated and the oxygen plasma treated carbon fiber surfaces in the C1s spectra were quite different.

Table III presents the results of the C1s peak deconvolution analysis, showing a distinctive change of functional groups on the carbon fiber surface after the oxygen plasma treatment. It was found that the untreated carbon fiber sample was consisted of 72.5% $-\text{C}-\text{C}-$, 8.5% $-\text{C}-\text{N}$, 12.3% $-\text{C}-\text{OH}/-\text{C}-\text{O}-\text{C}$, 2.5% $-\text{C}=\text{O}$ and 4.3% $-\text{COOH}/-\text{COOR}$. The $-\text{C}=\text{O}$ and $-\text{COOH}/-\text{COOR}$ concentrations of the untreated carbon fiber surfaces experienced significant increases from 2.5% and 4.3% to 30.2% and 13.3% after oxygen plasma treatment for 3 min, and then reduced to 2.7% and 3.2% after oxygen plasma treatment for 7 min.

The results suggested that for the carbon fibers, the concentration of surface carbon functional component was significantly different before and after the oxygen plasma treatment. In other words, the oxygen plasma treatment could increase the density of carbonyl functional group and carboxylic and/or ester functional groups on the surface of carbon fiber.

Morphology analysis of carbon fibers surface

Longitudinal surface morphologies of the carbon fibers under study were investigated by AFM in tapping mode. A comparison of AFM images of the untreated and the oxygen plasma treated carbon fibers is shown in Figure 4. The images provide some clues about the properties of carbon fibers and composites. It is observed that fine striations running parallel to the fiber axis, due to the spinning process of the fiber precursor, on the untreated carbon fiber surface [Fig. 4(a)], the root mean square (RMS) roughness value of carbon fiber surface was

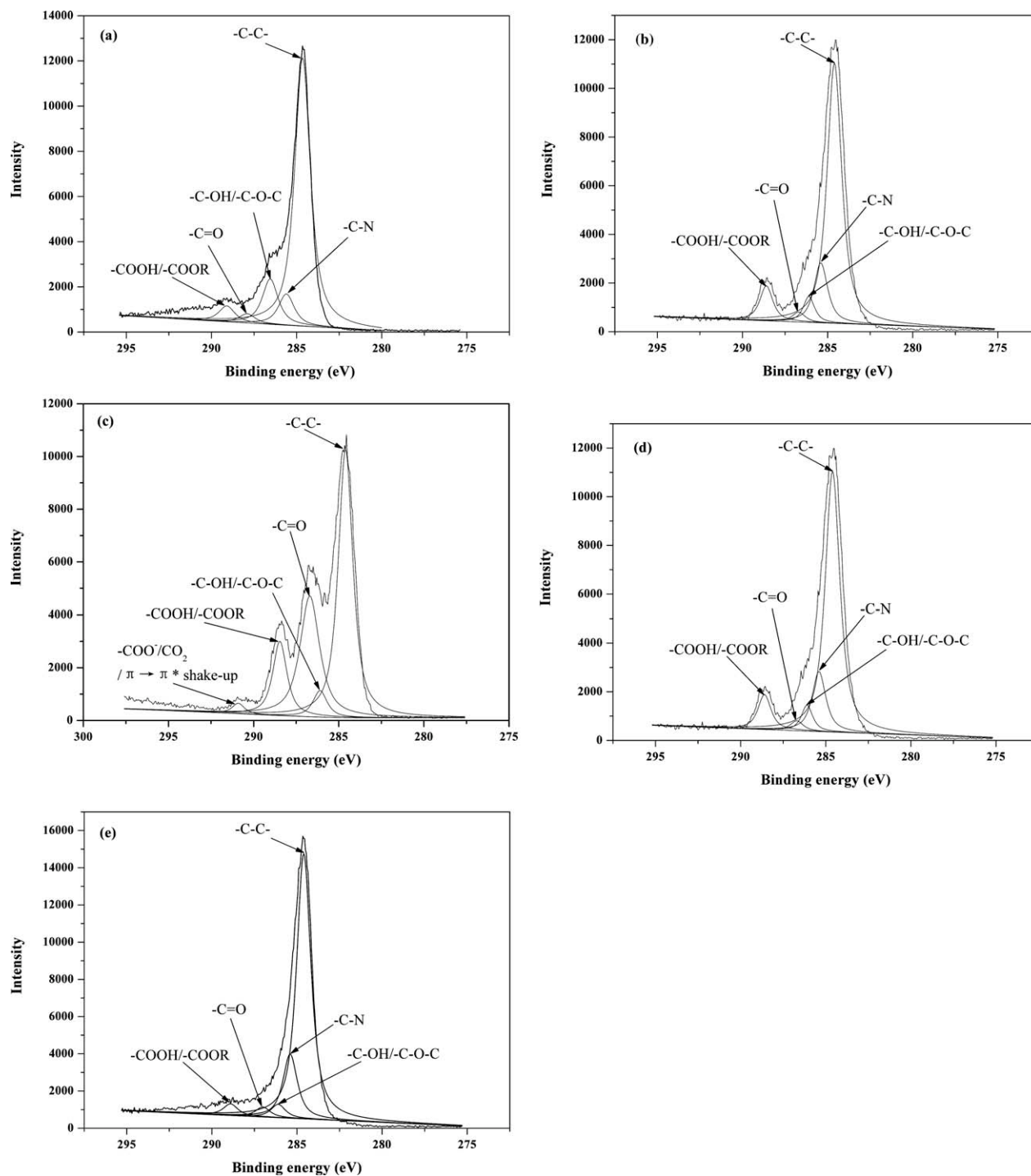


Figure 3 XPS C1s spectra of carbon fiber surfaces: (a) untreated; (b) plasma treated for 1min; (c) plasma treated for 3 min; (d) plasma treated for 5 min; (e) plasma treated for 7 min.

491.08 nm. After carbon fibers were oxygen plasma treated for 1, 3, and 5 min [Fig. 4(b-d)], the RMS roughness values of carbon fiber surface were 513.60, 536.65, and 640.30 nm, respectively, the change of RMS roughness values was very small. But after oxygen plasma treatment for 7 min, carbon fiber surface have clear ridges and striations running along fiber axis [Fig. 4(e)], the RMS roughness value

reached to 813.21 nm, the change of RMS roughness value was very notably.

The gradual increase of surface roughness on oxygen plasma treated fibers promotes more mechanical keying which enhances the interfacial bonding between the fibers and the resin. Removing a weak boundary layer initially present on the fiber surface is also believed to play a positive role during the

TABLE III
Correlative Functional Groups of Carbon Fibers

Samples	The concentration of correlative functional groups (%)					
	-C-C-	-C-N	-C-OH/-C-O-C	-C=O	-COOH/ -COOR	-COO ⁻ /CO ₂ /π→π* shake-up
Untreated	72.5	8.5	12.3	2.5	4.3	0
Plasma treated for 1 min	75.5	8.6	6.6	5.9	3.5	0
Plasma treated for 3 min	50.0	0	4.8	30.2	13.3	1.6
Plasma treated for 5 min	69.3	14.9	5.3	2.3	8.2	0
Plasma treated for 7 min	72.8	17.6	3.7	2.7	3.2	0

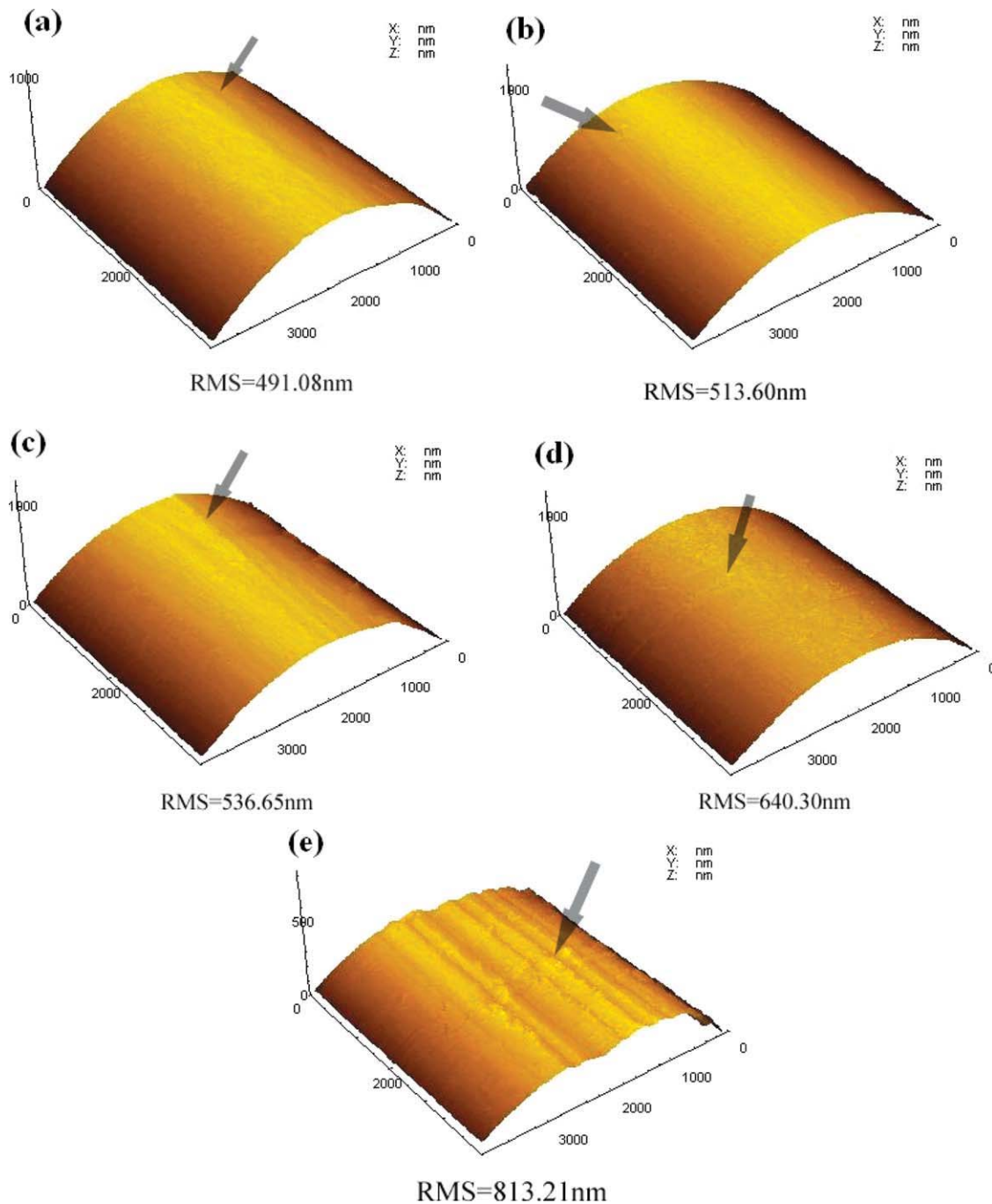


Figure 4 AFM images of carbon fibers: (a) untreated; (b) plasma treated for 1 min; (c) plasma treated for 3 min; (d) plasma treated for 5 min; (e) plasma treated for 7 min. [Color figure can be viewed in the online issue, which is available at www.interscience.wiley.com.]

TABLE IV
Surface Free Energy (mN/m) of Carbon Fibers

Samples	Contact angle (°)		Surface free energy (mN/m)		
	Water	Diiodomethane	γ_s^p	γ_s^d	γ_s
Untreated	64.52	62.65	15.92	27.05	42.97
Plasma treated for 1 min	54.82	52.78	19.40	32.71	52.11
Plasma treated for 3 min	40.11	48.57	27.21	35.07	62.28
Plasma treated for 5 min	58.11	50.40	16.81	34.05	50.86
Plasma treated for 7 min	59.91	47.05	15.00	35.90	50.90

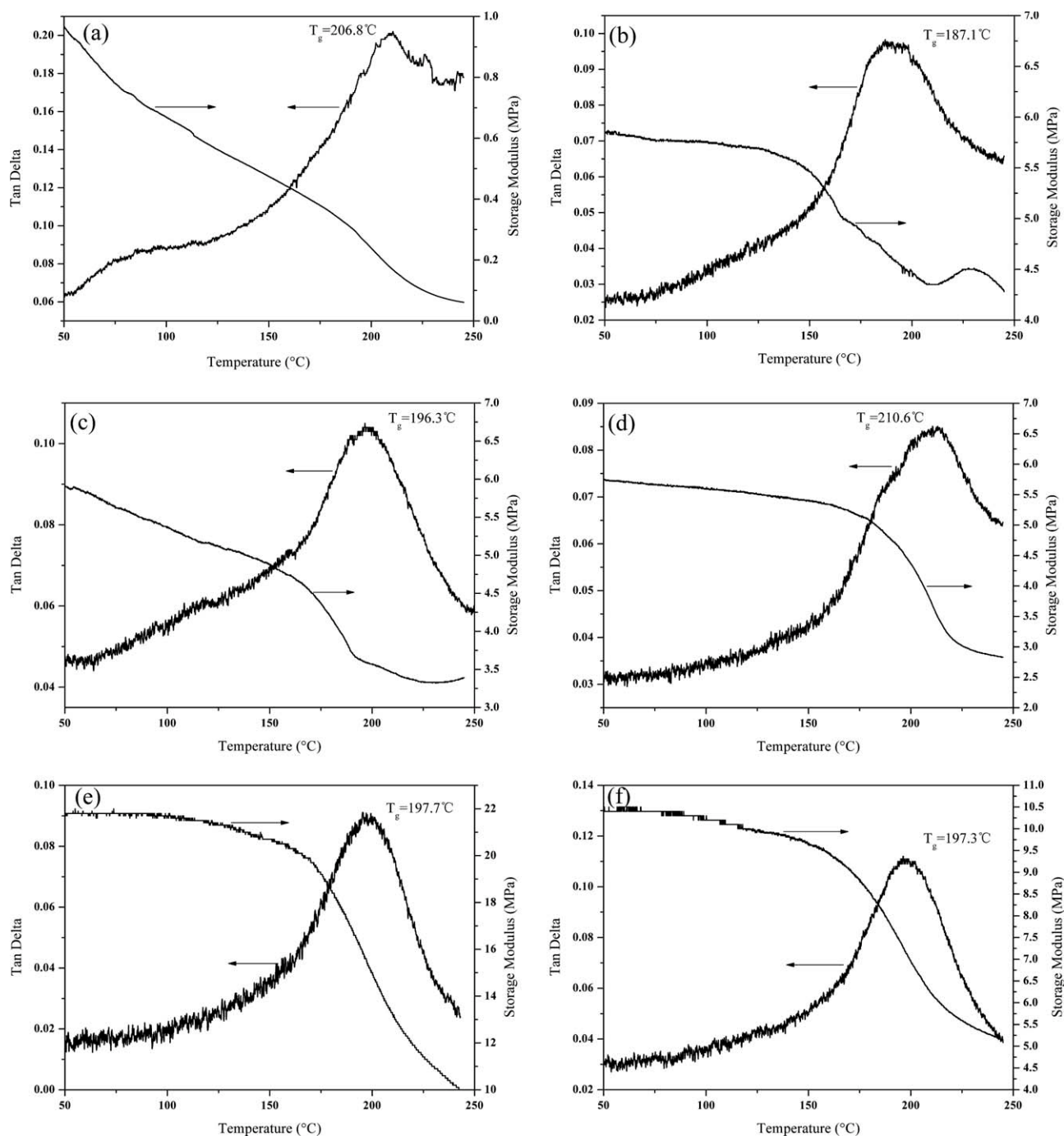


Figure 5 Storage modulus and tangent delta for epoxy matrix and composites: (a) epoxy matrix; (b) untreated; (c) plasma treated for 1min; (d) plasma treated for 3 min; (e) plasma treated for 5 min; (f) plasma treated for 7 min.

TABLE V
Interfacial Bonding Intensities and Loss Factor $\tan\delta$ of the Composites

	Epoxy matrix	Untreated	Oxygen plasma treated			
			1 min	3 min	5 min	7 min
V_f (%)	–	46.63	40.32	48.10	53.22	43.99
$\tan\delta_{\max}$	0.201	0.097	0.105	0.084	0.089	0.112
A	–	–0.100	–0.129	–0.199	–0.058	–0.010
α ($\times 10^{-3}$)	–	2.252	2.406	2.453	2.123	2.046

early stage of plasma treatments. Nevertheless, since plasma consists of various highly energetic species, exposure of fibers to the plasmas for an extended period of time could have a negative effect to the fiber strength.²⁰ Strong plasma treatments may increase the population of critical flaws on the carbon fiber surface and decrease its mechanical properties. As a result, the composites containing excessive plasma treated fibres may exhibit poorer mechanical properties.

Surface energy of carbon fibers

The contact angles and surface free energy of carbon fibers before and after oxygen plasma treatment are shown in Table IV. Table IV shows that after oxygen plasma treatment, the contact angles both of water and diiodomethane on carbon fiber decreased. The contact angles of water, the polar component and the dispersive component of surface free energy on the untreated carbon fibers were 64.52°, 15.92, and 27.05 mN/m, respectively, the total surface free energy was 42.97 mN/m. However, after oxygen plasma treatment for 3 min, the contact angles of water on the carbon fibers reduced to 40.11°, the polar component of surface free energy and the total surface free energy increased to 27.21 and 62.28 mN/m, respectively, the percentage of the total surface energy increased was 44.9, while the contact angles of diiodomethane and the dispersive component of surface free energy have been little changed. This could be explained by that the oxygen plasma treatment changed the property and constitution of carbon fibers, increased some polar functional groups concentration on the carbon fibers surface as already shown by XPS measurements (Table III) and increased the surface roughness (Fig. 4), which can enhance the surface free energy and the reactivity. The increased surface free energy affects the fiber surface wettability, and also influences the reactivity and interfacial properties of the fibers deeply.²¹

Interfacial bonding intensities of carbon fiber/epoxy composites

Typical DMTA curves at 2°C/min scan rate and 1 Hz oscillating frequency for epoxy matrix and carbon fiber/epoxy composites are illustrated in Figure 5.

Table V presents the interfacial bonding intensities A , α and loss factor $\tan\delta$ of the unidirectional carbon fiber/epoxy composites.

As shown in Table V, interfacial bonding intensity A decreased from –0.100 to –0.199 and α increased from 2.252×10^{-3} to 2.453×10^{-3} after oxygen plasma treatment for 3 min. However, when the plasma treatment time increased from 3 min to 7 min, the A increased from –0.199 to –0.010 and α decreased from 2.453×10^{-3} to 2.046×10^{-3} , respectively. When the carbon fiber was treated by oxygen plasma for 3 min, the composites present minimum A and maximum α value. The strong interactions between the fiber and the matrix at the interface tends to reduce macromolecular mobility in the fiber surface environment, as compared to mobility at other regions in the matrix, this fact reduces $\tan\delta$ and hence A , and a lower A value is the indicative of a higher degree of fiber-matrix interaction or adhesion at the interface.¹⁵ For the same reason, the higher α means the higher degree of interaction between the fiber and the matrix.

The ILSS of carbon fiber/epoxy composites

The effect of plasma treatment on ILSS for the unidirectional carbon fiber/epoxy composites is given in Figure 6.

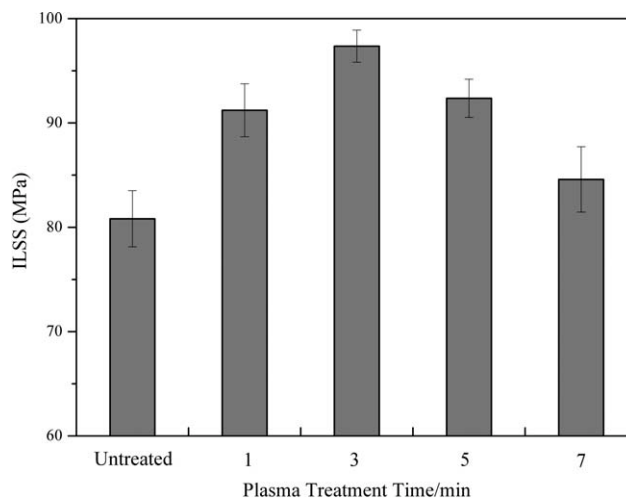


Figure 6 Effect of plasma treatment on ILSS of composites.

As can be seen, there is an initial increase in the ILSS of carbon fiber/epoxy composites. After oxygen plasma treatment for 3 min, the ILSS of composites reached the maximum 97.4 MPa, 21% more than that of the untreated fibers. As plasma treatment time increased from 3 to 7 min, the ILSS value decreased. Investigation by XPS, DCAA and DMTA proved that the density of carbonyl functional group and carboxylic and/or ester functional groups on the surface of carbon fiber were increased after oxygen plasma treatment, which lead to the surface free energy of carbon fibers increased notably. The increased surface energy of carbon fibers helped to increase the surface energy difference between carbon fiber and epoxy and thus improved the wettability of fiber with epoxy. On the other hand, AFM analysis revealed that the surface roughness on oxygen plasma treated fibers increased gradually, which promotes more mechanical keying between the fibers and the resin. As a result, the interface adhesion of carbon fiber/epoxy composites was strengthened and ILSS was increased. The results conform to the DMTA measurement results very well.

CONCLUSION

In this article, the chemical and physical modification of oxygen plasma-treated carbon fiber-reinforced epoxy composites was studied. It was found that the surface characteristics of the carbon fiber were greatly influenced by the oxygen plasma treatment, some active functional groups concentration such as —C=O and —COOH/—COOR were increased on the surface of carbon fiber. AFM analyses show that oxygen plasma treatment increased the roughness of the carbon fiber surface. The DCAA and DMTA verified that the wettability and interfacial adhesion ability of carbon fiber were

enhanced. As a result, the composites composed of carbon fiber treated with oxygen plasma can obtain the highest ILSS value.

References

1. Kim, N. I.; Kang, H. M.; Hong, Y. T.; Yoon, T. H. *J Adhes Sci Technol* 2002, 16, 1825.
2. Hélène, L.; Charles, M.; Hansen, A. *Carbon* 2007, 45, 2859.
3. Oku, T.; Kurumada, A.; Kawamata, K.; Inagaki, M. *J Nucl Mater* 2002, 303, 242.
4. Montes-Morán, M. A.; Van Hattum, F. W. J.; Nunes, J. P.; Martínez-Alonso, A.; Tascón, J. M. D.; Bernardo, C. A. *Carbon* 2005, 43, 1778.
5. Kang, H. M.; Kim, N. I.; Yoon, T. H. *J Adhes Sci Technol* 2002, 16, 1809.
6. Xu, B.; Wang, X. S.; Lu, Y. *Appl Surf Sci* 2006, 253, 2695.
7. Cara, L.; Weitzsacker, M.; Xie; Drzal, L. T. *Surf Interface Anal* 1997, 25, 53.
8. Li, H.; Liang, H.; He, F.; Huang, Y.; Wan, Y. Z. *Surf Coat Technol* 2009, 203, 1317.
9. Xuezhong, Z.; Yudong, H.; Tianyu, W. *Appl Surf Sci* 2006, 253, 2885.
10. Zhu, L.; Wang, C. X.; Qiu, Y. P. *Surf Coat Technol* 2007, 201, 7453.
11. Bin, L.; Chang-Rui, Z.; Feng, C.; Si-Qing, W.; Bang, C.; Jun-Sheng, L. *Mater Sci Eng A* 2007, 471, 169.
12. Jin, Z.; Zhang, Z. Q.; Meng, L. H. *Mater Chem Phys* 2006, 97, 167.
13. Fukunaga, A.; Ueda, S.; Nagumo, M. *Carbon* 1999, 37, 1081.
14. Liu, L.; Song, Y. J.; Fu, H. J.; Jiang, Z. X.; Zhang, X. Z.; Wu, L. N.; Huang, Y. D. *Appl Surf Sci* 2008, 254, 5342.
15. Fang, G.; Zhao, Z. Z.; Wei, M. L.; Feng, H. S.; Hui, J. Z. *Tribol Int* 2009, 42, 243.
16. Lu, C.; Chen, P.; Yu, Q.; Ding, Z. F.; Lin, Z. W.; Li, W. *J Appl Polym Sci* 2007, 106, 1733.
17. Zhang, C. S.; Chen, P.; Sun, B. L.; Li, W.; Wang, B. C.; Wang, J. *Appl Surf Sci* 2008, 254, 5776.
18. Chen, P.; Zhang, C. S.; Zhang, X. Y.; Wang, B. C.; Li, W.; Lei, Q. Q. *Appl Surf Sci* 2008, 255, 3153.
19. Ibarra, L.; Panos, D. *J Appl Polym Sci* 1998, 67, 1819.
20. Tao, C. *J Ind Technol* 1999, 15, 1.
21. Papakonstantinou, D.; Amanatides, E.; Mataras, D.; Ioannidis, V.; Nikolopoulos, P. *Plasma Process Polym* 2007, 4, S1057.